Constraining AGN Properties in Recently Quenched Galaxies with Low-Count Chandra Observations

Lauranne Lanz[1], Katherine Alatalo[2], Kate Rowlands[2,3], K. Decker French[4], Sofia Stepanoff[1,5], Louis Miller[1], Dean Klunk[1,6], Joe Petrecca[1]

[1]TCNJ, [2] Space Telescope Science Institute, [3] John Hopkins University, [4] U. of Illinois, Urbana-Champaign, [5] Georgia Tech, [6]Hampton University

Identifying Shocked Post-Starburst Galaxies

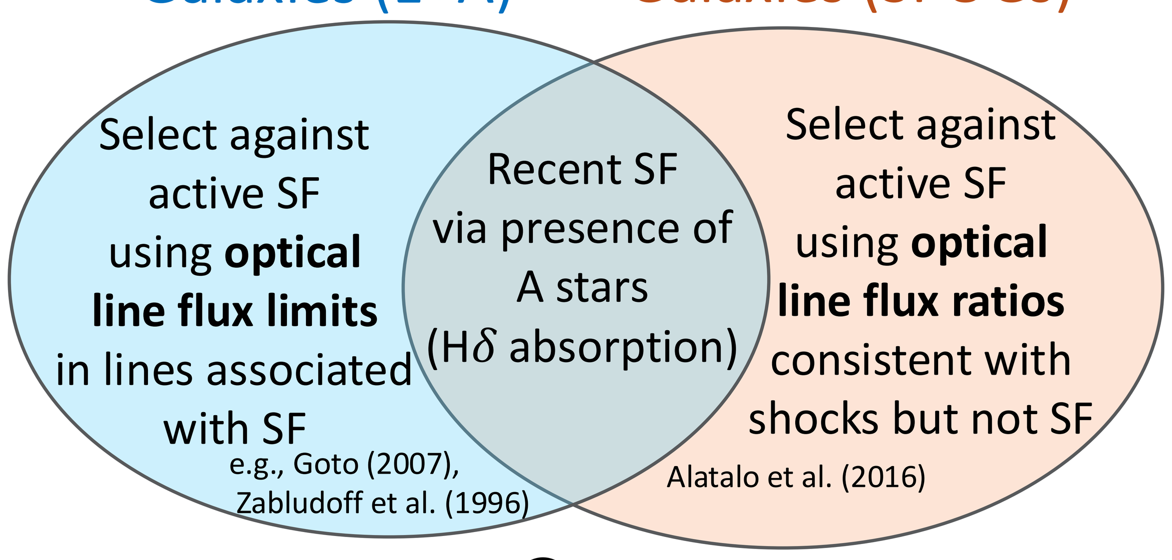

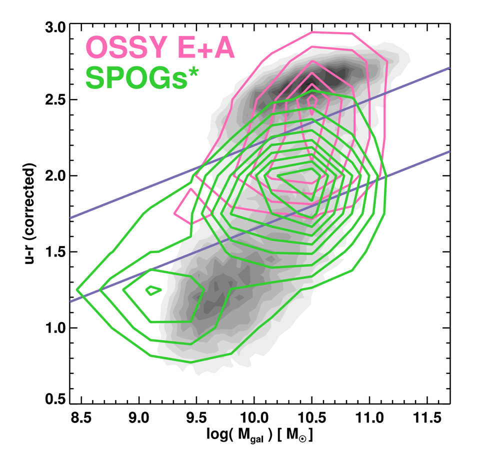

Fig. 1: Color-mass diagram showing SPOGs tend to be bluer than E+A.

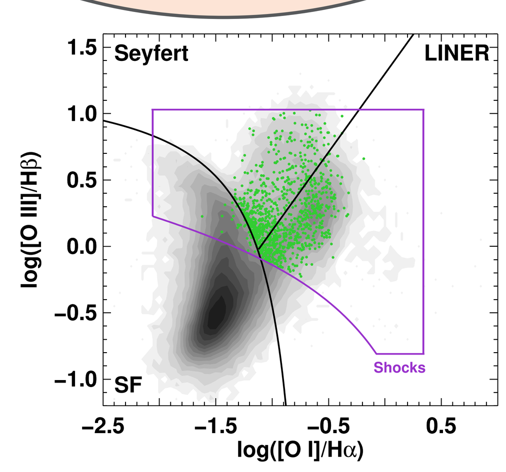

Fig. 2: A line diagnostic diagram used to select SPOGs (green dots).

Figures from Alatalo et al. (2016)

Fig. 3: On-going observations with TCNJ's 27in telescope of lowest redshift subset (z<0.02) to check whether regions not covered by SDSS fiber also show optical colors consistent with post-starburst population. Circle is 20'' overlaid on a 60 min observation of SPOG264. Inset in lower left shows SDSS image of this galaxy.

Work by Dean Klunk, being continued by Emily Harms

Forward Modeling Methodology

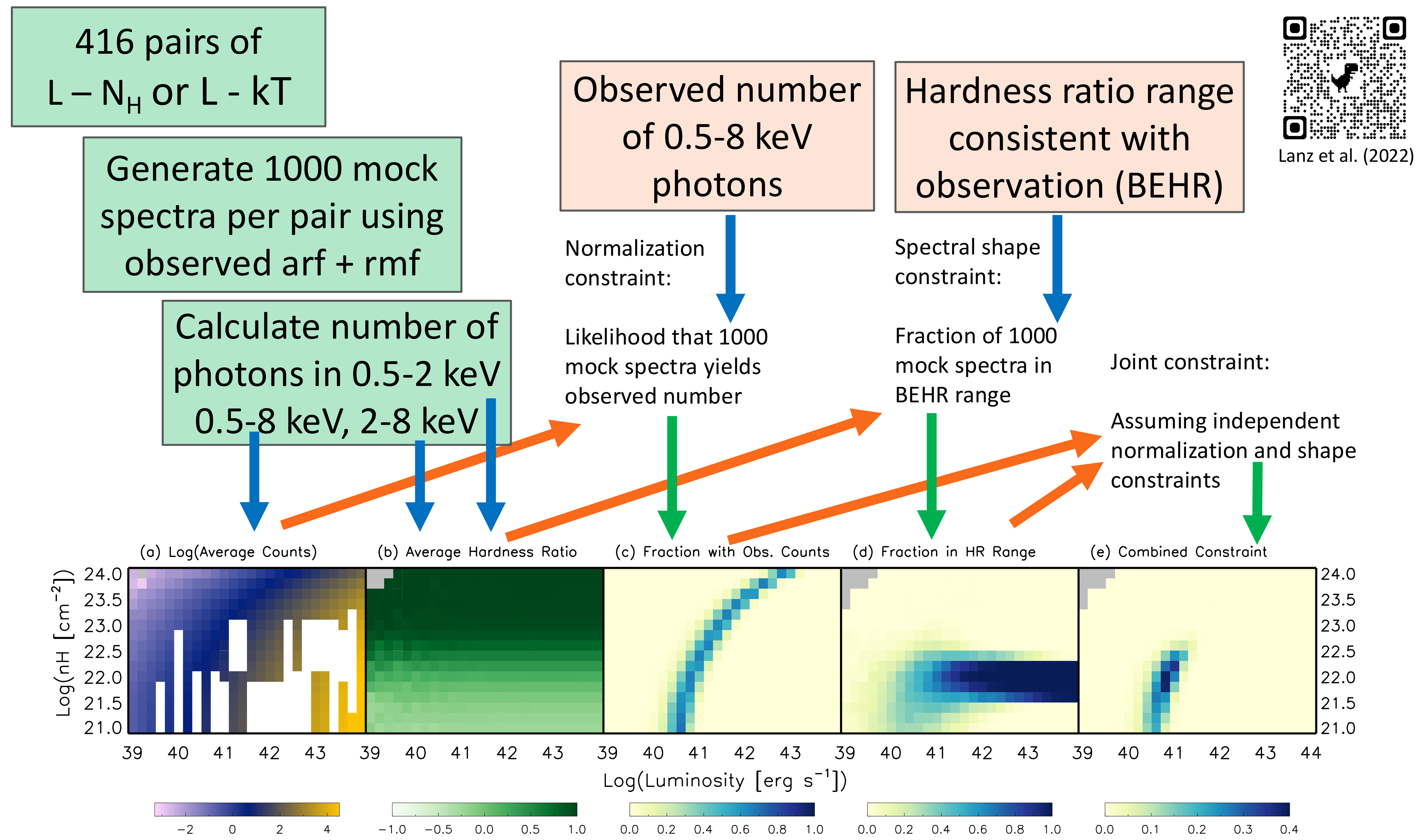

Code development and revision led by undergraduates Sofia Stepanoff and Joe Petrecca. Testing led by undergraduate Dean Klunk.

Pros: **provides *individualized* constraints in 2-D parameter space**, applicable to other models (e.g., APEC), adjustable range, number of models, and statistical power (based on number of mock spectra)

Limitations: can only rule *out* models based on statistical likelihood, not compare which of two good models is better

Chandra Observations

46 SPOGs have Chandra observations:

12 targeted/analyzed in Lanz et al. (2022)

2 others targeted; 32 serendipitously observed

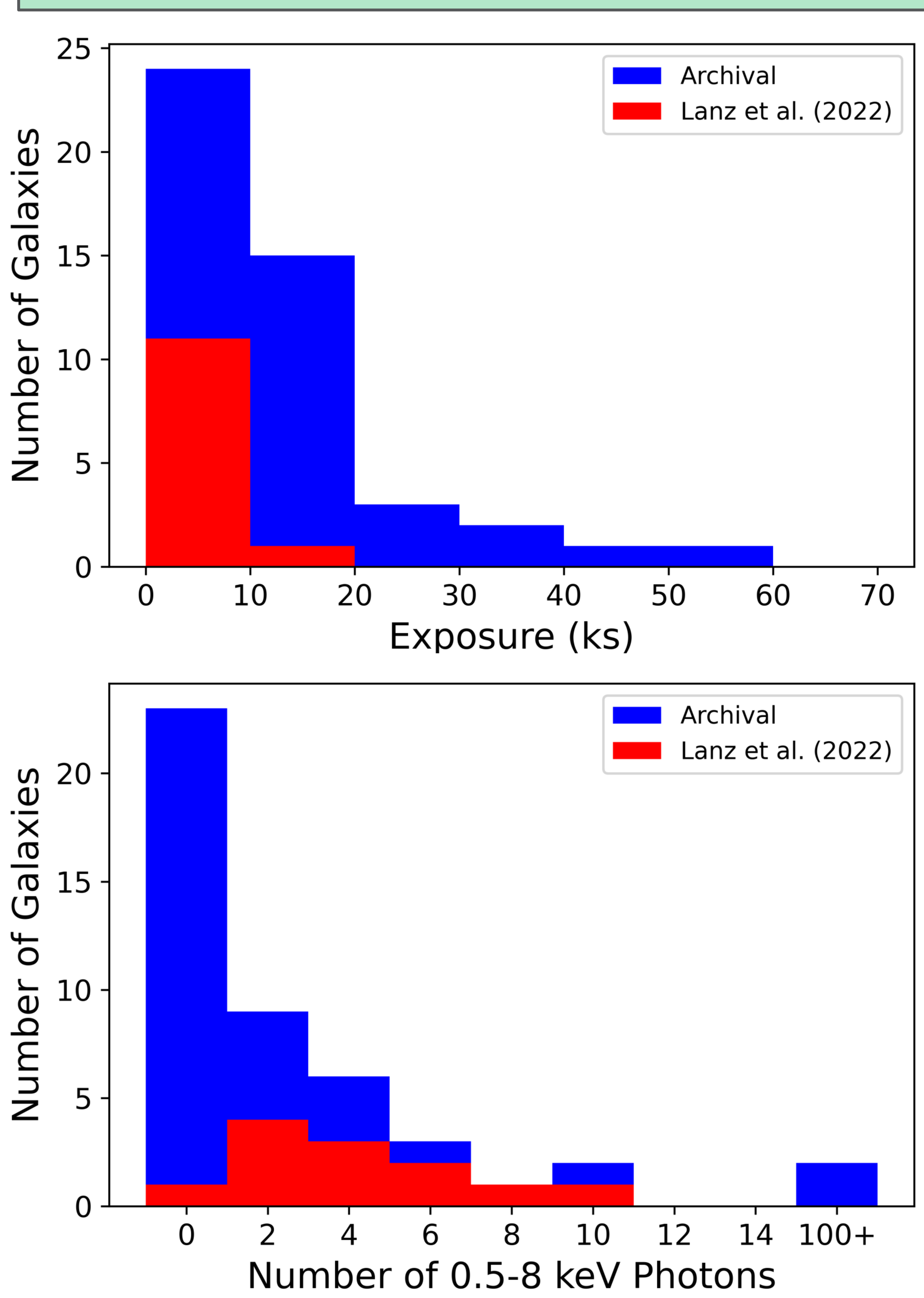

Fig. 4: Most observations are short (under 10 ks) and most have 0-2 photons. Two sources (SPOGs 105 and 111) have more than 100 photons, enough for a spectral fit.

Data collection and early analysis led by undergraduates Louis Miller

Results

Frequency of X-ray nuclear Emission

When 1 or more photons is measured in a 2'' aperture centered on the post-starburst galaxy, its significance is determined based on the expected background emission in that aperture. Background emission primarily depends on the exposure length and detector chip.

Significance	Lanz et al. (2022)		New Archival		Total	
above Bkg	Number	Percent	Number	Percent	Number	Percent
≥99%	7	58%	12	35%	19	41%
90% - 99% (Marginal)	2	17%	3	9%	5	11%
≥90%	**9**	**75%**	**15**	**44%**	**24**	**52%**
<90% (1-2 photons)	3	25%	3	9%	6	13%
No photons	0	0%	16	47%	16	35%

The Lanz et al. (2022) subset was selected from the subset of SPOGs observed with CARMA and IRAM, requiring a FIRST and WISE counterpart as well as CO(1-0) detection. While the detection rate of nuclear X-ray emission is lower in the serendipitous survey, the **frequency of nuclear X-ray emission** is still **elevated**.

Nature of X-ray Emission

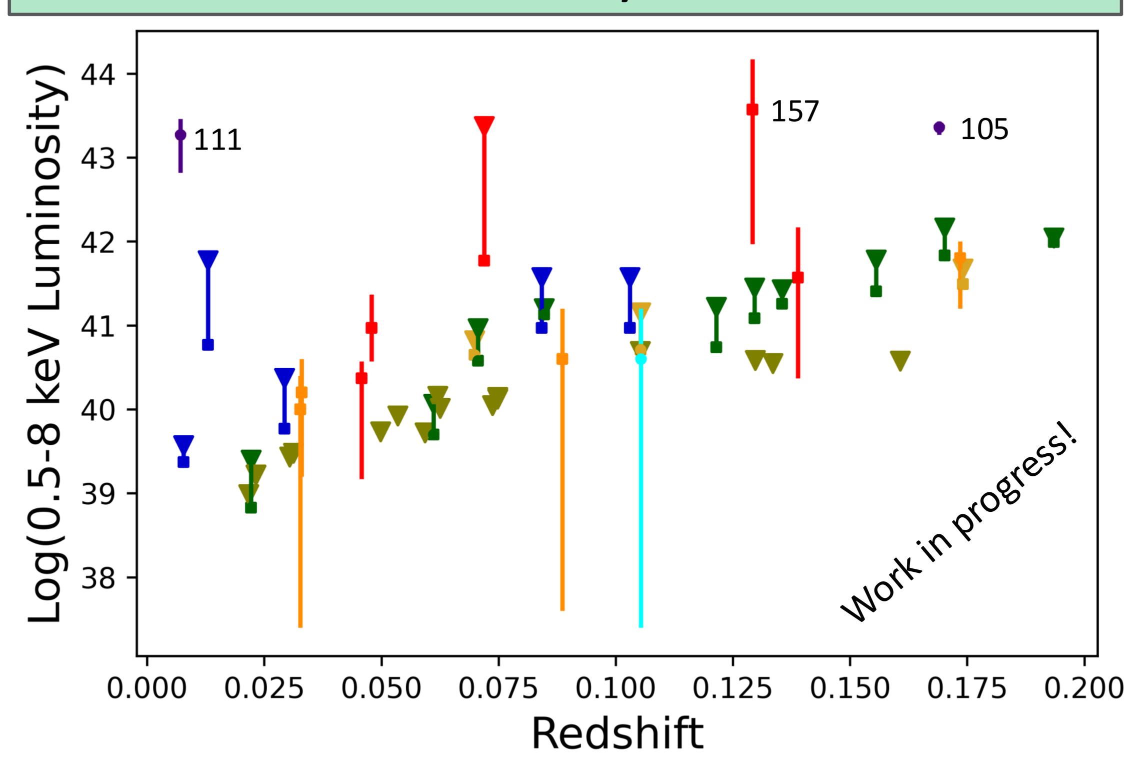

Fig. 6: Constraints on luminosities for these galaxies. Lanz et al. (2022) subset: Forward Modeling PL/APEC, and 1-2 photons

New archival sources: Spectral fits, Forward Modeling PL/APEC, 1-2 photons, and no photons

Comparison of Forward Modeling and Spectral Fit

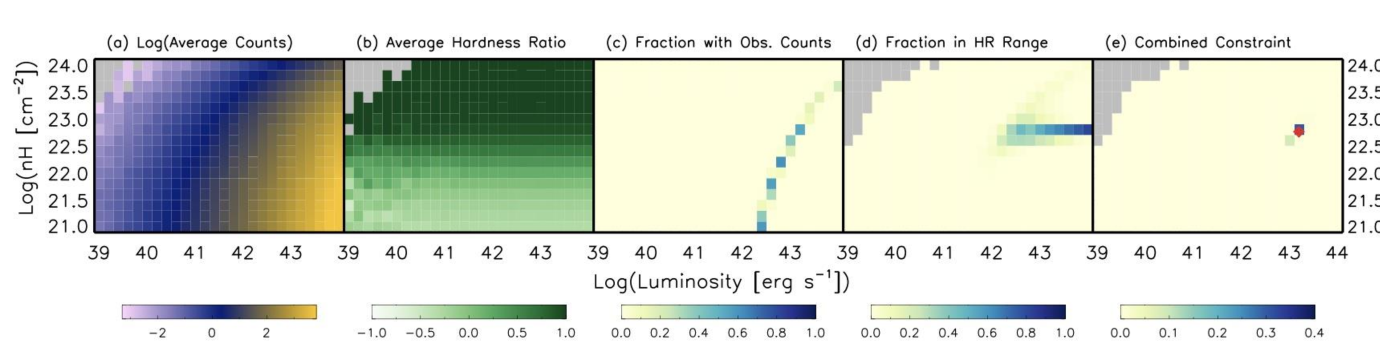

Fig. 5: Forward modeling results for SPOG105, with 110 photons. The red marker in panel e shows the results of fitting the spectrum with an absorbed power-law, which found consistent results. We have likewise seen consistent results for SPOGs 157 and 253 (10, 6 Chandra photons) and deeper XMM spectra.

High frequency of activity suggests transition process feeds the SMBH. Low luminosities, however, indicate that AGN most likely at best prevent resurgence of star formation rather than driving the quenching.

Other applications: investigating background source potential for point sources in HCG57

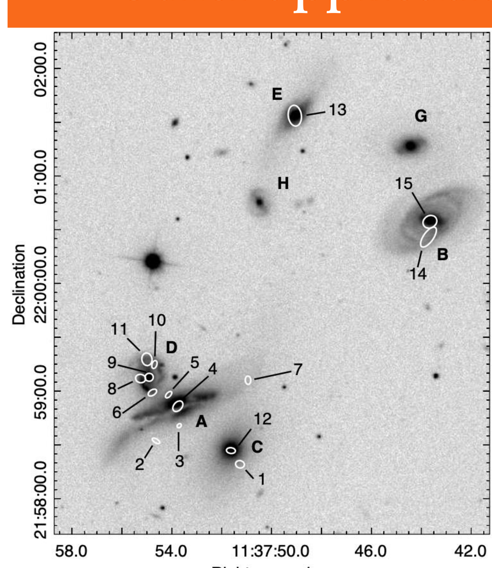

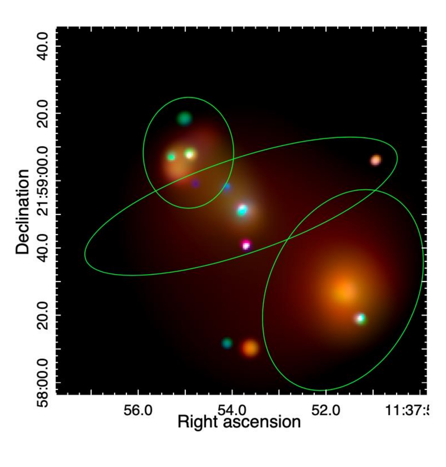

Fig. 7: Figs. 5 (right) and 10(left) from O'Sullivan et al. (2024), showing locations of X-ray point sources in HCG57. Fig. 10 shows their location relative to SDSS *g* emission. Fig. 5 shows Chandra Emission from HCG57A, C, and D at 0.5-1, 1-2, and 2-7 keV (RGB).

Source	net counts (0.5-7 keV)	$L_{0.5-7keV}$ (10^{40} erg s^{-1})	log($N_{H,FM}$) (cm^{-2})	kT_{FM} (keV)	$L_{0.5-7keV,FM}$ (10^{40} erg s^{-1})
on S3					
1	79.4±10.1	1.14±0.14	22±0.2	-	$2.19^{+0.57}_{-0.80}$
2	9.9±4.0	$0.13^{+0.06}_{-0.05}$	24^d	-	<34.85
3^a	84.2±9.5	1.27±0.14	22.4±0.01	-	$3.48^{+0.90}_{-0.72}$
4	339.6±20.8	$13.59^{+4.88}_{-2.81}$	-	-	-
5^b	33.8±6.8	$0.46^{+0.10}_{-0.09}$	22.3±0.3	-	$1.39^{+0.80}_{-0.51}$
6	17.2±5.9	0.25±0.08	>21.8	-	$0.87^{+54.4}_{-0.53}$
7	16.2±4.9	$0.23^{+0.07}_{-0.06}$	<22.4	-	<0.55
8	30.5±7.8	0.44±0.10	<21.8	-	$0.35^{+0.21}_{-0.07}$
9	90.6±10.9	$1.44^{+0.18}_{-0.17}$	-	-	-
10	9.3 ±4.5	$0.14^{+0.06}_{-0.05}$	<22	-	<0.22
11^c	13.6±6.4	$0.21^{+0.08}_{-0.07}$	<21.8	-	<0.35
12	26.7±7.43	$0.36^{+0.10}_{-0.09}$	-	0.6	$0.40^{+0.23}_{-0.24}$
on S2					
13	76.7±10.3	$1.33^{+1.67}_{-1.65}$	-	>1.5	$1.00^{+0.26}_{-0.21}$
14	36.8±7.8	$0.66^{+0.13}_{-0.12}$	<21.8	-	$0.87^{+0.22}_{-0.32}$
15	18.0±6.3	$0.31^{+0.10}_{-0.09}$	<21.8	-	$0.35^{+0.21}_{-0.12}$

^{a}0.72'' from SSTSL2 J113753.73+215841.1

^{b}1.32'' from SSTSL2 J113754.08+215859.1

^{c}0.9'' from SSTSL2 J113755.01+215916.8

^{d}The parameter is unconstrained, so only the value with highest probability is shown

Absorbed power-laws consistent with sources: 1-3, 5-7, 14
Higher absorption of 1, 3, 5 and 6 may suggest background AGN rather than associated ULX

Both absorbed power-law and APEC are consistent (at 95% confidence) with source properties for: 8, 10, 11, 15

Only APEC is consistent with source properties: 12, 13
Located centrally so may represent peak of hot gas emission in the galaxies

References and Acknowledgements

Alatalo, A. et al. (2016), ApJS, 224, 38
Goto, T. (2007), MNRAS, 381, 187
Lanz, L. et al. (2019), ApJ, 870, 26
Lanz, L. et al. (2022), ApJ, 935, 29
O'Sullivan, E. et al. (2024), submitted to ApJ
Zabludoff, A. et al. (1996), ApJ, 466, 104

LL acknowledge support from NASA grants 80NSSC20K0050, 80NSSC22K0798, and G02-21107X. We also acknowledge use of the ESLA high performance computing cluster at TCNJ, funded in part under NSF grant numbers OAC - 1826915 and OAC - 2320244.